



Blast and tensile properties of tantalum/niobium lined SiC/SiC composite tubes for nuclear cladding

Chang LI, Hong-lei WANG, Ya-ping YANG, Quan-chao GU, Xing-heng YAN, Xin-gui ZHOU

Science and Technology on Advanced Ceramic Fibers and Composites Laboratory,
College of Aerospace Science and Engineering,
National University of Defense Technology, Changsha 410073, China

Received 8 March 2022; accepted 9 May 2022

Abstract: The mechanical performances such as tensile strength and blast property of metal lined SiC/SiC composite cladding tubes were investigated. Nb or Ta was selected as liner material, and the SiC/SiC composite layer was fabricated by winding and different precursor impregnation and pyrolysis (PIP) processes. The tensile strengths of different tube samples were measured at room temperature (RT) and 1200 °C, respectively. The blast property was investigated through the maximum water pressure of tubes. And the fracture microstructures were observed by SEM. The highest tensile strength at RT was 150.7 MPa. The blast strength was enhanced with the PIP process increasing from 1 to 4 cycles and the tube of 4 PIP cycles had the highest water pressure of 34.7 MPa. Compared with the metal tubes, the multi-layer structure improved tensile and blast properties significantly. The different processes such as PIP cycles and pyrolytic carbon (PyC) coating were important factors to enhance the mechanical performances of SiC/SiC-based tubes. However, the retention rate of tensile strength was only 18.5% at 1200 °C.

Key words: SiC/SiC composite; tantalum/niobium liner; tensile strength; blast property

1 Introduction

In recent decades, the Zr-based alloys have been widely used as fuel cladding in nuclear cores because of their excellent performance in irradiation environments. However, the degradation of Zr-based alloys in extreme accidents such as reactivity insertion accident (RIA) and loss-of-coolant accident (LOCA) will lead to dramatic rise of temperature, which has attracted much attention recently [1–3]. Meanwhile, the process called zirconium–water reaction will occur when the temperature is higher than 1000 °C. In addition, this process is highly exothermic and releases an excessive amount of hydrogen gas. Therefore, a conception called accident tolerant fuel (ATF) cladding has been proposed as the substitution of

Zr-based cladding tubes [4–6].

The continuous SiC fiber-reinforced SiC matrix composite (SiC/SiC) is a candidate material for ATF cladding, because of its high strength, excellent stability at high temperature and oxidation resistance, good irradiation resistance and neutron absorption cross-section [7–9]. For the nuclear application, the generation-III SiC fiber has high degree of crystallinity, near-stoichiometry, high-temperature resistance, and oxidation resistance. The Hi-Nicalon-S and Tyranno-SA3 SiC fibers are the most popular, because they do not contain B that will have transmutation in irradiation [10,11]. The production process is another important factor that influences the SiC/SiC composite performance, including chemical vapor infiltration (CVI) [12], polymer impregnation and pyrolysis (PIP) [13], melting infiltration (MI) [14] and nano-infiltration

and transient eutectic (NITE) [15]. For example, KATOH et al [16] used Tyranno SA3 as reinforcement and polyvinylsilane (PVS) pyrolyzed at 1750–1800 °C to fabricate high-crystallization and low-C residual SiC/SiC composite which could maintain stability in the ion irradiation of 10 dpa and 600 °C, and the strength decreased slightly in the ion irradiation of 40 dpa and 800 °C. Through research of NITE SiC/SiC composite in the radiation environment, KISHIMOTO et al [17] found that the SiC fiber and matrix had a good stability in dual ion irradiation. These methods are targeted to fabricate SiC/SiC composite with a pure constituent, high crystallinity and density that can be considered a benefit for radiation stability.

Although the SiC/SiC composite has a great potential in the nuclear application, the structure, fabrication, and performances of SiC/SiC composite tubes still need extensive research. Different cladding prototypes have been proposed and fabricated. For instance, in General Atomics, several kinds of SiC-based cladding tubes with CVI as well as the bulk SiC ceramic and SiC/SiC composite layer with a thickness of 1.2–2.1 mm and a length of 900 mm were designed [18]. And in the Westinghouse, a similar SiC-based cladding prototype was fabricated by winding and CVI processes, and the bending strength in neutron irradiation of 5 dpa was evaluated [19]. At the same time, in Korean Atomic Energy Research Institute, three-layer SiC/SiC composite tubes were fabricated with winding, CVI and CVD processes, and the strength changes with winding patterns were simulated [20]. A cladding prototype using the so-called sandwich multilayer structure with a thickness of less than 1 mm was designed by CEA. The tubes' outer and inner layers were weaved by Hi-Nicalon or Tyranno SA3 at 60°, and the interlayer was made by high-temperature resistance metals such as niobium or tantalum [21]. By virtue of the NITE process, in the University of Tokyo, tubular SiC/SiC composite was fabricated, whose density was higher than 95% and conductivity was evaluated in RT and 1000 °C [22].

In general, the SiC/SiC composite was regarded as an excellent candidate for the next generation of cladding material. However, the structure design, production processes, and properties of SiC/SiC composite tubes need

in-depth exploration. In this work, the metal lined SiC/SiC composite tubes with the two-layer structure were fabricated. The inner layer was high-temperature resistant metal, and the outer layer was SiC/SiC composite prepared by winding and PIP processes. What's more, the tensile and blast properties under different processes and measuring conditions were investigated.

2 Experimental

2.1 Sample fabrication

A series of tube samples with different procedures were prepared to evaluate the tensile and blast properties of metal lined SiC/SiC composite tubes. With relatively high neutron absorption cross-section and high-temperature resistance, the tantalum and niobium may be appropriate in nuclear applications. Therefore, in this work, these two kinds of metals were chosen as the liner materials, and their tube samples were listed separately for comparison with metal lined SiC/SiC composite tubes.

The metal lined SiC/SiC composite tube samples with bilayer structure and the tube samples with different processes are listed in Table 1. Firstly, the tantalum or niobium tubes were fabricated by spinning as the inner layer of composite tubes. Then, the SiC fibers of KD-SA were wound on these metal dappers periodically with a 45° winding angle. It is noteworthy that the SiC fibers for the winding process were distinguished as pyrolytic carbon (PyC) coated and uncoated, and their SiC/SiC composite tube samples are differentiated as two groups correspondingly. Finally, the densification process of SiC/SiC composites was achieved by precursor infiltration and pyrolysis (PIP) and entire plasma-enhanced chemical vapor deposition (PECVD). The technological parameters of PECVD are listed in Table 2.

Table 1 Metal tubes and SiC/SiC-based composite tubes

Tube sample	Structure	SiC fiber	Process
Ta/Nb	Monolayer of metal	–	Spinning
Ta/Nb-SiC/SiC	Bilayer	Uncoated	Winding+PIP+CVD
Ta/Nb-SiC/PyC/SiC	Bilayer	PyC-coated	Winding+PIP+CVD

Table 2 Important parameters of PECVD processes

Reactant gas	Airflow of MS/ (mL·min ⁻¹)	Heating rate/ (°C·min ⁻¹)	Carrier gas	Airflow of H ₂ / (mL·min ⁻¹)	Deposition temperature/°C
Modified silanes	100	5	H ₂	200	750

2.2 Characterization

The tube samples with different processes were cut as short tubes with a length of 200 mm, and 5 short tubes were selected as one group for measurement. According to ASTM C1773-13, two steel poles were inserted in tube ports for supporting samples, aluminum alloy scale-boards were stuck outside the tube ends with a 20° dip angle. Furthermore, the tensile property was measured by tensile testing machine (Instron 8801) at room temperature and high temperature (1200 °C), respectively. The loading rate was 10 N/s, while the heating rate was 10 °C/min. For simulating working conditions in nuclear cores, inner pressure resistance should be taken into account. The tube ports of burst testing samples were plugged with steel thin pipe tightly, and then connected with a water booster system and pressure sensor. At the same time, the enhanced rate of water pressure was 1 MPa/s, with the pressure ranging from 0.1 to 50 MPa.

The microstructures of tube fractures were observed by scanning electron microscope (SEM, model HITACHI S-4800). In addition, the phase analysis was characterized by X-ray diffraction and energy disperse spectroscopy.

3 Results and discussion

3.1 Tensile properties

Figure 1(a) shows Nb lined SiC/SiC composite tube samples after tensile testing and corresponding fractures at room temperature. Due to the grasp of a testing machine, the SiC fiber bundles of tube ends were scattered. At the fracture region of samples, the Nb liner had serious deformation and a large amount of SiC fibers were debonded and pulled out from the SiC/SiC composite layer. For the tube samples after tensile testing at high temperature, as displayed in Figs. 1(b, c), some cracks appeared at the fractures of the metal liner and SiC/SiC composite layer along with the winding directions. Compared with the samples at room temperature, less debonding and pulling-out of SiC fibers could

be observed in high-temperature tested samples. However, a new layer with lower strength and lower density could be observed at the surface of Nb tubes or between the metal liner and SiC/SiC composite layer.



Fig. 1 Nb lined SiC/SiC composite tubes after tensile testing at room temperature (a) and 1200 °C (c), and Nb tube after tensile testing at 1200 °C (b)

The tensile strength could be calculated based on equation below:

$$\sigma = L/A, A = \pi(R^2 - r^2) \quad (1)$$

where σ represents the average tensile strength of tube samples, L represents the maximum load when a tube sample fails in the testing process, A represents the cross-section area calculated based on the geometric dimensions of tube samples. Additionally, the inner (r) and outer diameter (R) of tube samples could be measured by a digital vernier calliper.

The average tensile strengths of Nb tubes and Nb lined SiC/SiC composite tubes are shown in Fig. 2. At room temperature, the tensile strength of Nb lined SiC/SiC composite tubes with PyC coating was 150.7 MPa which was much higher than that of the metal tubes and uncoated tubes. Similar phenomenon could be observed in high-temperature tested sample that the PyC coating samples had the highest tensile strength of

27.9 MPa. The SiC/SiC composite layer not only provided entire strength of tubes but also improved the tensile strength significantly. However, the strength of coating samples only retained 18.5% in 1200 °C-tested sample. The error bars indicate standard deviations of the measured strength, and the values for high-temperature tested samples presented more obvious dispersion than those for room-temperature tested samples.

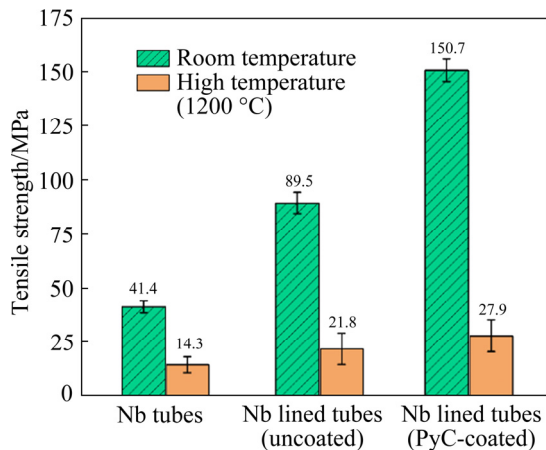


Fig. 2 Tensile strength of Nb tubes and Nb lined SiC/SiC composite tubes at RT and 1200 °C

As shown in Fig. 3(a), the stress–strain curve of Nb lined SiC/SiC composite tubes was significantly different from the typical yield curve of niobium tubes. Moreover, an elastic stage could be observed in the initial period, and then tensile load increased gradually until sample failure. This curve may be influenced by the combined effects of pseudo-plastic from SiC/SiC composite layer and niobium liner. It is noteworthy that, as shown in the insert of Fig. 3(a), the curve of Nb lined SiC/SiC composite tubes without PyC coating was significantly different from PyC coated samples. After the elastic stage in the initial period, the stress of uncoated samples descended suddenly and presented a jagged curve in the end period. That is to say, the failure process of tube samples is brittle fracture.

The stress–strain curve of Nb lined SiC/SiC composite tubes in 1200 °C-tested sample, as shown in Fig. 3(b), displayed the typical pseudo-plastic fracture. The stepped descent of the curve could reflect the debonding and pulling-out of SiC bundles. This process consumed much fracture energy. For the uncoated samples, although similar variation tendency could be observed, the maximum stress was lower and the descent degree

of the curve was much more extremely than coated samples, indicating that less fracture energy was consumed in the tensile process.

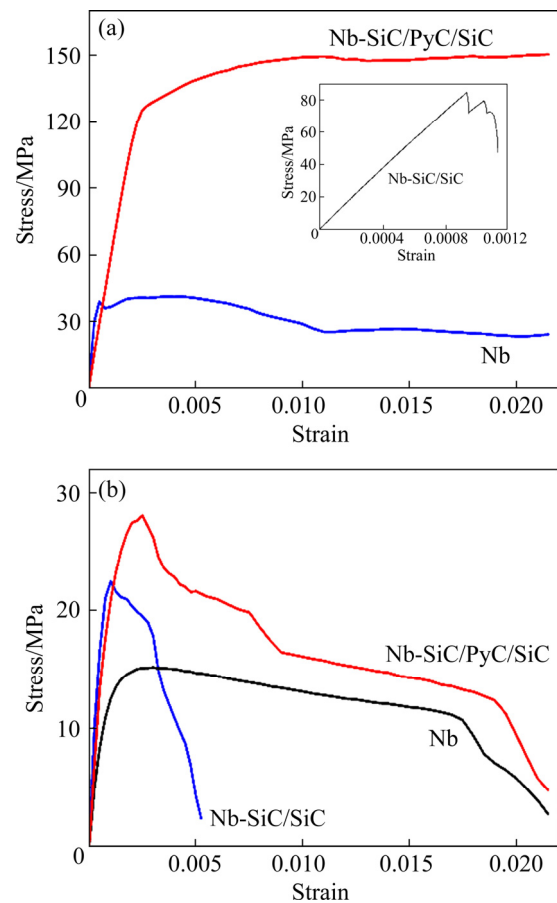


Fig. 3 Stress–strain curves of tubes tested at room temperature (a) and 1200 °C (b)

Figures 4(a, b) show fracture microstructures of Nb lined SiC/SiC composite tube samples uncoated and coated with PyC, respectively. Obviously, the pulling-out fibers in PyC coated samples were much longer than those in uncoated ones. These phenomena demonstrate that PyC coating modified the defects of the SiC fiber surface and deflected the growing crack in the matrix (see Fig. 4(e)) due to the weak interface effect from the lamellar structure of PyC. In 1200 °C-tested samples, a similar phenomenon of fibers debonding and pulling-out could be observed and a corresponding typical pseudo-plastic fracture could be obtained, but the tensile strength could not retain efficiently. That is to say, some more important factors have caused the property degradation. As shown in Fig. 4(f), the new layer between Nb liner and SiC/SiC composite after high-temperature tension had a low density and

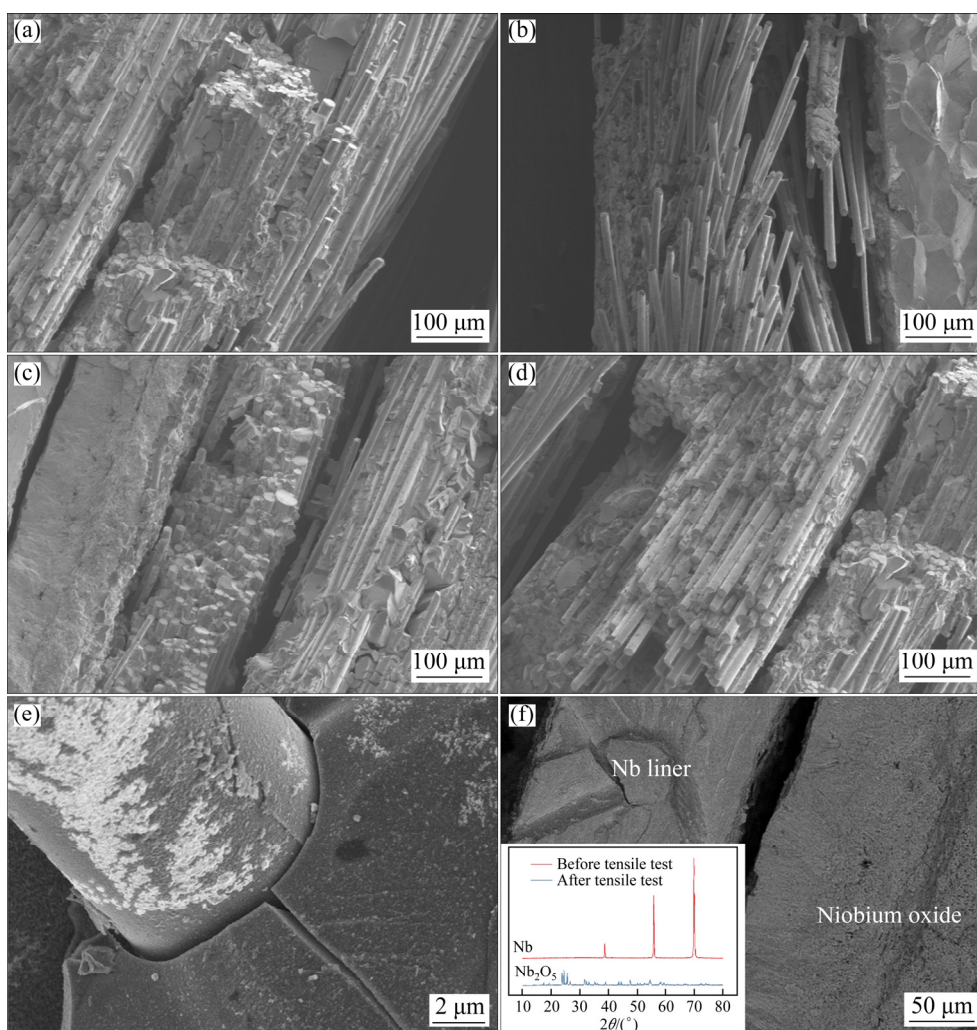


Fig. 4 Fracture microstructures of Nb lined SiC/SiC tubes uncoated (a, c) and coated with PyC (b, d) tested at room temperature (a, b) and 1200 °C (c, d), crack deflection in SiC/SiC composite tubes (e), and gap between Nb liner and oxide layer and XRD patterns (f)

porosity structures. According to the XRD analysis, the new layer contained a large amount of niobium oxide dominated by Nb_2O_5 , as shown in the insert of Fig. 4(f). The volume expansion of the oxide layer and falling-off from the metal liner might lead to dramatic damage between the Nb liner and SiC/SiC composite, and then reduce the tensile strength tremendously.

3.2 Blast properties

As shown in Fig. 5, several groups of Ta lined SiC/SiC composite tube samples with different PIP cycles were blasted in water pressure testing. Most fractures were located in the middle of the tubes. It could also be observed that some fractures were located at the end of tubes and the cracks grew along the axial direction. The tube samples with 3 and 4 PIP cycles presented slight bending

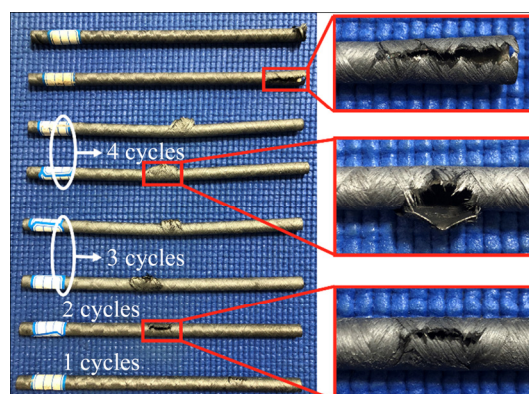


Fig. 5 Ta liner SiC/SiC composite tubes after water pressure test

deformation after burst, and their fractures were more open than 1- and 2-cycle samples.

The maximum water pressure value is regarded as the ultimate strength in water boost

process to evaluate the blast property of tubes. As shown in Fig. 6, the Ta tube had the lowest strength of 12 MPa. The SiC/SiC composite layer enhanced the strength of tubes significantly. And the PyC coating also improved the blast property obviously. The strength increased with PIP cycles, and the 4 PIP-cycle tubes had the highest strength of 34.7 MPa. As shown by the error bars, the measured values with more PIP cycles were more concentrated. From the density variation of Ta lined tubes shown in Fig. 6, the PIP process caused the higher density and lower porosity of the SiC matrix, which might lead to the improvement of blast strength. In addition, Fig. 7(a) presents the relative blast curves of SiC/SiC composite tubes in different PIP cycles. As shown in Fig. 7(b), the maximum water pressure increased with the enhanced water pressurization rate from 2 to 4 MPa/s, meaning that the water pressurization rate also influenced the blast strength of tubes.

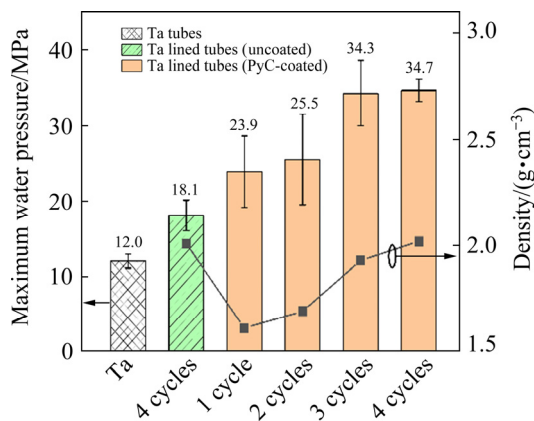


Fig. 6 Maximum water pressure of Ta tubes and Ta lined SiC/SiC composite tubes in different PIP cycles

The fracture microstructures of Ta liner SiC/SiC composite tube samples after blast testing are shown in Fig. 8(a). An obvious debonding could be observed between the SiC/SiC composite layer and metal liner. A lot of SiC fibers adhered to metal liner and were debonded from SiC/SiC composite layer transversely. It could be observed that a great number of SiC fibers and bundles were pulled out from the SiC matrix and most fiber lengths of pulling out were greater than 200 μm . The higher magnification figure, as shown in Fig. 8(b), reveal that the cracks branched and deflected and then stopped growing at the interface between the fibers and matrix. For PyC coated tube samples, the coating modified the surface of SiC fibers and

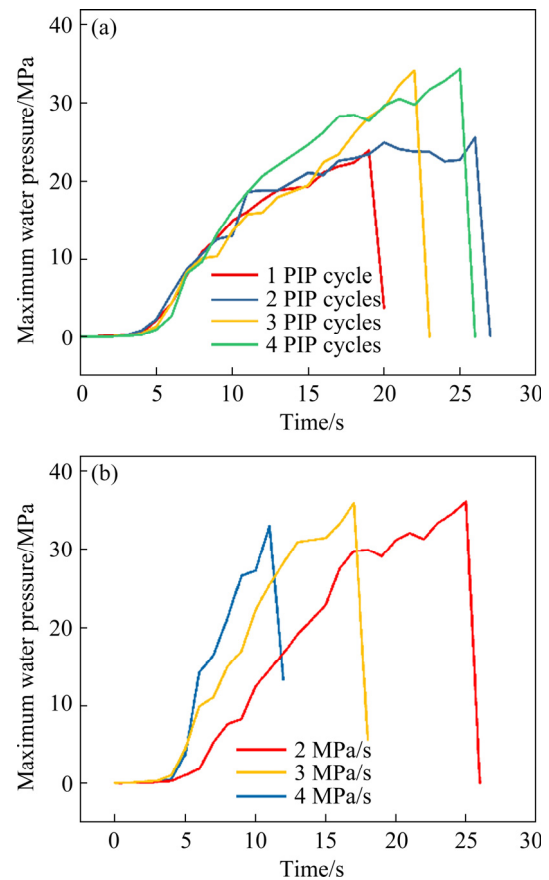


Fig. 7 Blast curves of Ta liner SiC/SiC composite tubes in different PIP cycles (a), and blast curves of 4-cycle tubes at different water pressurization rates (b)

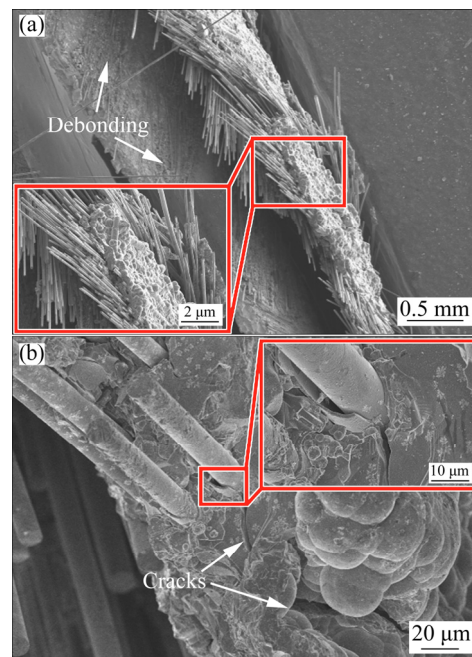


Fig. 8 Debonding of Ta liner and SiC/SiC composite layer and feature of pulling-out SiC fibers (a); cracks in Ta liner SiC/SiC composite tubes after blast testing and feature of crack branches and deflections (b)

weak interface formed, which were beneficial to improving mechanical properties of composites and enhancing the blast strength.

4 Conclusions

(1) The highest tensile strength of metal lined SiC/SiC composite tubes was 150.7 MPa and the maximum water pressure of them was 34.7 MPa. At the same time, the bilayer structure with SiC/SiC composite layer improved the tensile and blast properties of the tubes. Furthermore, the PyC coating on SiC fibers enhanced the performance through modification of the brittle fracture behavior.

(2) The maximum water pressure was enhanced from 23.9 to 34.7 MPa with increasing the PIP cycles. In the process of more PIP cycles, the higher density and lower porosity of SiC matrix might trigger the improvement of blast strength.

(3) Although the tensile strength of metal lined SiC/SiC composite tubes was high at room temperature, the retention rate was merely 18.5% at 1200 °C. Meanwhile, the oxide layer formed in high-temperature atmosphere might cause dramatic performance reduction.

Acknowledgments

This work was supported by the National Key R&D Program of China (No. 2018YFB1900603) and the Natural Science Foundation of Hunan Province, China (No. 2020JJ4667).

References

- [1] CINBIZ M N, KOYANAGI T, SINGH G, KATOH Y, TERRANI K A, BROWN N R. Failure behavior of SiC/SiC composite tubes under strain rates similar to the pellet-cladding mechanical interaction phase of reactivity-initiated accidents [J]. *Journal of Nuclear Materials*, 2019, 514: 66–73.
- [2] QIU B, WANG J, DEND Y, WANG M, WU Y, QIU S Z. A review on thermohydraulic and mechanical-physical properties of SiC, FeCrAl and Ti₃SiC₂ for ATF cladding [J]. *Nuclear Engineering and Technology*, 2020, 52(1): 1–13.
- [3] LIU Z, LI Y F, SHI D W, GUO Y L, LI M, ZHOU X B, HUANG Q, DU S Y. Reprint of: the development of cladding materials for the accident tolerant fuel system from the Materials Genome Initiative [J]. *Scripta Materialia*, 2017, 143: 129–136.
- [4] TERRANI K A. Accident tolerant fuel cladding development: Promise, status, and challenges [J]. *Journal of Nuclear Materials*, 2018, 501: 13–30.
- [5] MOTTA A T, COUET A, COMSTOCK R J. Corrosion of zirconium alloys used for nuclear fuel cladding [J]. *Annual Reviews of Materials Research*, 2015, 45: 311–343.
- [6] KO J, KIM J W, MIN H W, KIM Y, YOON Y S. Review of manufacturing technologies for coated accident tolerant fuel cladding [J]. *Journal of Nuclear Materials*, 2022: 153562.
- [7] BRAUN J, SAUDER C, LAMON J, BALBAUD-CELERIER F. Influence of an original manufacturing process on the properties and microstructure of SiC/SiC tubular composites [J]. *Composites Part A: Applied Science and Manufacturing*, 2019, 123: 170–179.
- [8] NODA T. Advanced SiC–SiC composites for nuclear application [M]//*Handbook of Advanced Ceramics and Composites: Defense, Security, Aerospace and Energy Applications*. Cham: Springer, 2020: 641–666.
- [9] AGARWAL S, DUSCHER G, ZHAO Y, CRESPILO M L, KATOH Y, WEBER W J. Multiscale characterization of irradiation behaviour of ion-irradiated SiC/SiC composites [J]. *Acta Materialia*, 2018, 161: 207–220.
- [10] TAKEDA M, IMAI Y, ICHIKAWA H. Thermal stability of SiC fiber prepared by an irradiation-curing process [J]. *Composites Science and Technology*, 1999, 59: 793–799.
- [11] SUGIMOTO M, SHIMOO T, OKAMURA K. Reaction mechanism of silicon carbide fiber synthesis by heat treatment of polycarbonylsilane fibers cured by radiation: I-evolved gas analysis [J]. *Journal of the American Ceramic Society*, 1995, 78(4): 1013–1017.
- [12] KATOH Y, OZAWA K, HINOKI T, CHOI Y, SNEAD L L, HASEGAWA A. Mechanical properties of advanced SiC fiber composites irradiated at very high temperatures [J]. *Journal of the Nuclear Materials*, 2011, 417: 416–420.
- [13] KATOH Y, KOTANI M, KISHIMOTO H, YANG W, KOHYAMA A. Properties and radiation effects in high-temperature pyrolyzed PIP-SiC/SiC [J]. *Journal of Nuclear Materials*, 2001, 289: 42–47.
- [14] ESFEHANIAN M, GUNSTER J, MOZTARZADEH F. Development of a high temperature C_f/XSi₂–SiC(X=Mo, Ti) composite via reactive melt infiltration [J]. *Journal of the European Ceramic Society*, 2007, 27: 1229–1235.
- [15] KOYANAGI T, KATOH Y, TERRANI K A, KIM Y, KIGGANS J O, HINOKI T. Hydrothermal corrosion of silicon carbide joints without radiation [J]. *Journal of Nuclear Materials*, 2016, 481: 226–233.
- [16] KATOH Y, OZAWA K, SHIH C, NOZAWA T, SHINAVSKI R J, HASEGAWA A, SNEAD L L. Continuous SiC fiber, CVI SiC matrix composites for nuclear applications: properties and irradiation effects [J]. *Journal of Nuclear Materials*, 2014, 448: 448–476.
- [17] KISHIMOTO H, OZAWA K, HASHITOMI O, KOHYAMA A. Microstructural evolution analysis of NITE SiC/SiC composite using TEM examination and dual-ion irradiation [J]. *Journal of Nuclear Materials*, 2007, 367–370: 748–752.
- [18] DECK C P, KHALIFA H E, SAMMULI B, HILSABECK T, BACK C A. Fabrication of SiC–SiC composites for fuel cladding in advanced reactor designs [J]. *Progress in Nuclear Energy*, 2012, 57: 38–45.
- [19] GRIFFITH G W. US department of energy accident resistant SiC clad nuclear fuel development [C]//*Enlarged Halden Programme Group Meeting 2011*. Idaho National Lab. (INL),

- Idaho Falls, ID (United States), 2011: INL/CON-11-23186.
- [20] KIM Daejong, LEE Hyun-Geun, PARK Ji Yeon, KIM Weon-ju. Fabrication and measurement of hoop strength of SiC triplex tube for nuclear fuel cladding applications [J]. Journal of Nuclear Materials, 2015, 458: 29–36.
- [21] DENG Y B, LIU M H, QIU B W, YIN Y, GONG X, HUANG X, PANG B, LI Y C. Design and evaluation of an innovative LWR fuel combined dual-cooled annular geometry and SiC cladding materials [J]. Nuclear Engineering and Technology, 2021, 53: 178–187.
- [22] SHIMODA K, PARK J S, HINOKI T, KOHYAMA A. Microstructural optimization of high-temperature SiC/SiC composites by NITE process [J]. Journal of the Nuclear Materials, 2009, 386–388: 634–638.

核用钽/铌内衬 SiC/SiC 复合材料管件的 拉伸与耐压性能

黎 畅, 王洪磊, 杨雅萍, 顾全超, 闫星亨, 周新贵

国防科技大学 空天科学学院 先进陶瓷纤维及其复合材料重点实验室, 长沙 410073

摘 要: 研究金属内衬的 SiC/SiC 复合材料管件的抗拉强度和爆炸特性等力学性能。采用铌或钽为内衬层, 通过缠绕及不同的 PIP 工艺制备一系列 SiC/SiC 复合材料管件。在室温与 1200 °C 下测量不同管件的抗拉强度, 通过测量最大耐水压强度表征管件的爆炸特性, 并利用扫描电镜观察断口显微形貌。结果发现, 室温下金属内衬 SiC/SiC 复合材料管件的抗拉强度可达 150.7 MPa; 随着 PIP 周期从 1 增加到 4, 管件的爆炸性能增加, 4 个 PIP 周期的管件最大耐水压强度可达 34.7 MPa。与单层结构的金属管件相比, 由 SiC/SiC 复合材料层与金属内衬结合的管件具有更好的拉伸与耐压性能。PIP 周期与热解炭涂层等不同工艺是提升金属内衬 SiC/SiC 复合材料管件力学性能的重要因素。然而, 在 1200 °C 时管件的抗拉强度保留率仅为 18.5%。

关键词: SiC/SiC 复合材料; 钽/铌内衬; 抗拉强度; 爆炸特性

(Edited by Bing YANG)